Enhanced Coupling of Subterahertz Radiation with Semiconductor Periodic Slot Arrays

Ramakrishnan Parthasarathy,[1] Alexei Bykhovski,[1] Boris Gelmont,[1,*] Tatiana Globus,[1]
Nathan Swami,[1] and Dwight Woolard[2]

[1]*Department of Electrical & Computer Engineering, University of Virginia, Charlottesville, Virginia 22904, USA*
[2]*U. S Army Research Laboratory, Army Research Office, Research Triangle Park, North Carolina 27709, USA*

(Received 3 November 2006; published 12 April 2007)

In this work, a theoretical study of the coupling of TM polarized subterahertz (THz) radiation with periodic semiconductor rectangular slot arrays was conducted, using InSb as an example. Simulation results showed that the structure with 4–12 μm thickness provides over a 20–30-fold increase in the electric field at slot edges in a nanosize region ($\sim$ 500 nm). The enhancement of the THz electromagnetic field extends across the slots and reaches peak values at the edges due to discontinuity effects. Because of the strong local electromagnetic field enhancement, the structure can potentially be used for the development of novel biophotonic sensors, leading to improved detection sensitivity.

DOI: 10.1103/PhysRevLett.98.153906 PACS numbers: 42.25.Bs, 42.25.Fx, 42.25.Gy, 42.79.Dj

Vibrational resonance spectroscopy in the terahertz (THz) gap or in the sub-THz range is a fast emerging technique for fingerprinting biological molecules and species with broad potential applications such as biomedicine or detection and identification of biological molecules. The technique is based on the specificity of spectroscopic signatures of molecules, which reflect absorption of THz radiation by the weakest hydrogen type bonds and nonbonded interactions within biological matter at characteristic resonance frequencies. Experimental and computational studies [1–3] have demonstrated the capability of THz spectroscopy as a very promising technique to discriminate between species. However, the problem of improving detection sensitivity of molecules with low absorption characteristics at THz remains an important issue. In order to increase the sensitivity and reliability of THz fingerprinting techniques, coupling of incident THz radiation to biological molecules has to be enhanced. One possible solution is to use periodic slot arrays. Such arrays were previously used for THz bandpass filters fabricated from lossy metal films deposited on dielectric membranes [4]. Experimental work on enhanced transmission is mostly available at optical and near-infrared frequencies for metallic periodic structures (gratings [5–8] and hole arrays [9–11]). Recently, it has been shown that waveguide resonance and diffraction are the main factors [8] contributing to enhanced transmission of narrow slot subwavelength metallic gratings. The phenomenon of extraordinary optical transmission (transmission efficiency exceeding unity when normalized to the surface of the holes) through hole arrays, first experimentally observed in Ag [9,10], has been attributed to the resonant tunneling of surface plasmons [10–15] through thin films. Recently, similar studies were done in the THz range with hole arrays in films made of metals (Ag-coated stainless steel [16], Al-coated Si wafers [17]) and doped semiconductors (Si [18] and InSb [19]). However, the observed transmission enhancement at THz in lossy metal foils with hole arrays is not well understood and a rigorous treatment is not provided [16,17] since the qualitative analysis relied on the dispersion of surface plasmons in a uniform film [20] that is inappropriate in the case of hole arrays.

In the THz region, interaction between radiation and metals is quite different from higher frequency regions due to the change in material dielectric properties. In the visible and near-IR regions, where frequencies are only slightly less than plasma frequency, the permittivities are predominantly real and negative (for example, at wavelength 1 μm, $\varepsilon_{\mathrm{Au}} = -51.4 + j1.6$), and metals are reflective. On the contrary, as we go down in frequency to the THz, the real part continues to be negative and large, but the dissipative imaginary part becomes larger, and hence metals are very conducting and absorbing (at wavelength 500 μm, $\varepsilon_{\mathrm{Au}} = -5.5 \times 10^4 + j8.5 \times 10^5$). Therefore, to reduce radiation losses, it is preferable to substitute metals with doped semiconductors with plasma frequencies in the low THz range. InSb with high electron mobility and low effective mass is most suited for this purpose, but still has a substantial absorbing imaginary part compared to the real component. The absorbing component requires the assumption of a small film thickness, which makes the InSb skin depth at both InSb-air interfaces larger than half the film thickness throughout our frequency range of interest. This renders the surface impedance boundary conditions for perfect conductors [21,22] to be unsuitable for our case. On the other hand, in contrast with the behavior of metals in short wavelength ranges, the Fourier expansion method for field diffracted from gratings [5] can be applied in the THz region for InSb films, since the imaginary permittivity component damps the Gibbs oscillations [23].

In this Letter, we study the mechanism of coupling of TM polarized THz radiation to the periodic semiconductor structure, consisting of a doped semiconductor film with rectangular slot arrays, using InSb as an example. Transmission properties of subwavelength slot arrays are funda-

mentally different from arrays of holes, since unlike hole arrays, a slot array can support propagating waveguide modes [24]. Thus, even in the absence of surface plasmon resonances, increased transmission and local electric field enhancement for TM incidence can be obtained through careful choice of materials and design of periodic slot array structures. We demonstrate that the enhancement of the THz electromagnetic field extends across the slots and reaches peak values at the edges because of discontinuity effects.

For modeling purposes, we consider a subwavelength array of slots with the periodicity in the x direction and extending all the way in the y direction. The z direction is perpendicular to the plane of incidence. Since the structural geometry is not altered in the y direction, it would suffice to analyze a one-dimensional periodic slot structure as shown in Fig. 1 with spacing (or periodicity) denoted by d, the slot width by s, and the thickness of the film by h. The structure was considered to be illuminated at normal TM incidence. The relative permittivity in the modulated medium ($0 < z < h$) was expressed as $e_{\mathrm{II}}(x)$, which was expanded as a Fourier series [5] with $(N + 1)$ modes,

$$e_{\mathrm{II}} = \sum_{n=0}^{N} e_n \cos(ngx), \tag{1}$$

where $g = \frac{2\pi}{d}$.

Projecting the coefficients of the pseudoperiodic electric and magnetic field functions, again on the $\cos(ngx)$ basis, and substituting in the coupled differential equations [5] obtained from Maxwell's equations for the fields inside the modulated medium, we obtain

$$V_{n,p}\kappa_p = -j\varepsilon_0\omega \sum_{m=0}^{N} (e_{\mathrm{II}})_{n-m} W_{m,p}, \tag{2}$$

$$W_{n,p}\kappa_p = \left(\frac{j}{\varepsilon_0\omega}\right) ng \sum_{m=0}^{N} mg \left(\frac{1}{e_{\mathrm{II}}}\right)_{n-m} V_{m,p} - V_{n,p}, \tag{3}$$

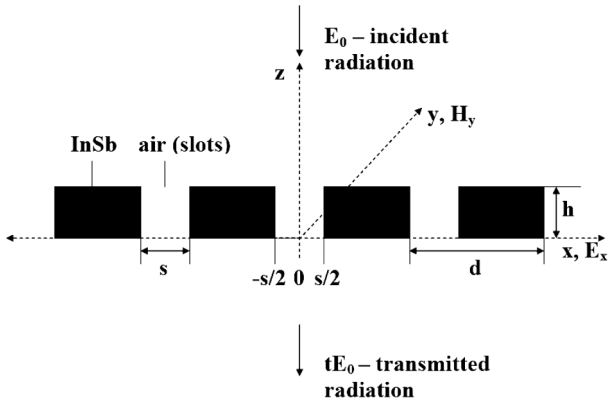

FIG. 1. The periodic rectangular slot array structure. The axes and the structure parameters (d—spacing, s—slot width, h—film thickness) are shown.

where $j = \sqrt{-1}$, ε_0 is the permittivity of free space and angular frequency is denoted by ω.

A coupled set of Eqs. (2) and (3) constitute an eigenvalue problem, which has $2(N + 1)$ solutions; κ_p represents the eigenvalues, i.e., propagation constants and $V_{n,p}$, $W_{n,p}$ are the eigenvectors, i.e., coefficients associated with the magnetic and electric fields, respectively. The total electric and magnetic fields were expressed as linear combinations of eigenmodes.

$$H_y^m = \sum_{p=1}^{2(N+1)} e^{\kappa_p z} A_p \left(\sum_{n=0}^{N} V_{n,p} \cos(ngx) \right), \tag{4}$$

$$E_x^m = \sum_{p=1}^{2(N+1)} e^{\kappa_p z} A_p \left(\sum_{n=0}^{N} W_{n,p} \cos(ngx) \right). \tag{5}$$

The electric field (E_x^t) in the transmitted medium ($z < 0$) was written as

$$E_x^t = tE_0 e^{-j(\omega/c)z} + \sum_{n=1}^{N} E_n^t \cos(ngx) e^{\eta_n z}, \tag{6}$$

where $\eta_n = \sqrt{(ng)^2 - (\frac{\omega}{c})^2}$, E_0 is the amplitude of the incoming wave, E_n is the complex mode amplitude of order n, and t is the transmission coefficient. In the medium of incidence ($z > h$), the electric field (E_x^i) was written as a superposition of forward and reflected components.

$$E_x^i = E_0(e^{-j(\omega/c)(z-h)} + re^{j(\omega/c)(z-h)}) + \sum_{n=1}^{N} E_n^i \cos(ngx) e^{\eta_n (h-z)}, \tag{7}$$

where r is the reflection coefficient. The magnetic fields were obtained from the electric fields through Maxwell's equations. At the two interfaces, Maxwell's boundary conditions, i.e., continuity of H_y and E_x were applied to constitute a linear system of equations that can be solved for the unknown field amplitudes in all the regions as well as t and r. Furthermore, the field amplitudes were substituted back into the respective equations to find the electric field enhancements at desired regions relative to the incidence.

For polar materials like InSb, the frequency dependence of the relative permittivity, $\varepsilon(\omega)$, includes terms describing the interaction of light with free carriers (Drude model [25]) and with the optical phonons [26]

$$\varepsilon(\omega) = \varepsilon(0) - \frac{\omega_p^2}{\omega(\omega + j\tau^{-1})}, \tag{8}$$

where $\varepsilon(0)$ is the static dielectric constant and is 16.8 for InSb, τ is the relaxation time of the electrons, and $\omega_p = \sqrt{\frac{N_d e^2}{\varepsilon_0 m^*}}$ is the plasma frequency. N_d is the charge carrier concentration, e is the electronic charge, and m^* is the

electron effective mass. The mobility of the carriers is related to the relaxation time by

$$\mu = \frac{e\tau}{m^*}. \tag{9}$$

The test frequency was chosen to be 14 cm^{-1}, since absorption peaks of interest to FT-IR transmission spectroscopy of biological molecules occur in this region. At room temperature (300 K), InSb has an electronic mobility [27] of 7.7×10^4 $cm^2\,V^{-1}\,s^{-1}$. The corresponding carrier concentration is 1.1×10^{16} cm^{-3}. From Eqs. (8) and (9), InSb was found to have a relative permittivity of $-242.9 + j160.5$. The modulated medium has a discontinuous permittivity function, which can only be perfectly represented by infinite modes. Convergence of transmission for all frequencies was obtained after employing a finite Fourier sum of modes (764 in our case). Convergence was also confirmed by considering only the real part of InSb permittivity and running the model to satisfy energy conservation requirements ($|t|^2 + |r|^2 = 1$). It is very difficult to achieve convergence using the Fourier expansion method with just the real part of the permittivity function. Since our region of interest in THz is 10–25 cm^{-1}, we had to choose a spacing that was less than the smallest wavelength of the incident radiation, i.e., 400 μm. Modeling was conducted for two different periodicity values, $d = 381$ and 251 μm. Because of the high absorbing part of InSb permittivity, the thickness (h) was chosen to be small. We considered three different thicknesses, 12, 6, and 4 μm.

The far-field transmission of the structure, $|t|$, was calculated as a function of frequency for two periodicities at different s values with $h = 12$ μm. The results at $d = 381$ μm are plotted in Fig. 2. The appearance of two far-field transmission peaks in Fig. 2 can be attributed to the periodic modulation of permittivity in our structure. The low level of transmission, due to the predominant metallic behavior of the structure in this frequency range, is still considerably higher than that obtained in the absence of slots (~ 0.04). The maximum transmission was around 0.15 for $d = 381$ μm and 0.22 for $d = 251$ μm. The far-field power transmission is approximately a factor of 14 above that without any slots. The overall transmission magnitude is higher for a smaller periodicity at the same s/d ratio, thickness and frequency. This increase in transmission points to the effect of slot interactions since at $d = 251$ μm the slots are closer to each other. Our assumption of a small film thickness ($h \ll \lambda$) forbids resonance peaks in the transmission characteristics.

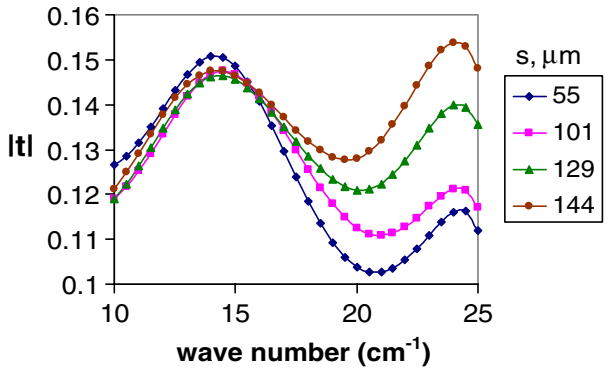

FIG. 2 (color online). Transmission, $|t|$, as a function of wave number for different values of s (μm). Here $d = 381$ μm, $h = 12$ μm.

Figure 3 is a plot of the electric field amplitudes at the incident interface [see Eq. (7)], $|\frac{E_x^i}{E_0}|$, as a function of the x coordinate with $s = 55$ μm and $h = 4$ μm, for the radiation frequency of 14 and 24 cm^{-1}. The strong electric field enhancement occurred within the submicron region around the slot edges, i.e., at discontinuities. Practically most of the fields were confined to the edges, i.e., sharp regions of the conducting medium. The enhancement at the edges was an order of magnitude higher than at other points within the slot. The decay into the metallic surface was more abrupt than into free space as expected. For the radiation frequency of 14 cm^{-1}, the maximum field enhancement was 33.3 at the incident interface and 31.8 at the outgoing interface for $h = 4$ μm. For $h = 6$ μm, these values were 27.7 and 25, respectively, and for $h = 12$ μm, 20.5 and 14.7, respectively. The half power width around the slot edges was $\sim$500 nm with maximum power enhancement $\sim$1100 for the $h = 4$ μm case. This region did not change much for the other h values. The enhancement also exists across the entire slot region, slightly decreasing in the z direction from the incident interface to the outgoing interface. It is higher at the radiation frequency of 14 cm^{-1} compared to 24 cm^{-1}.

In addition to $|\frac{E_x^i}{E_0}|$, we calculated the distribution of the z component of electric field, $|\frac{E_z^i}{E_0}|$, along the x coordinate, and found that both components behave approximately in accordance with edge effects [28] in our low frequency

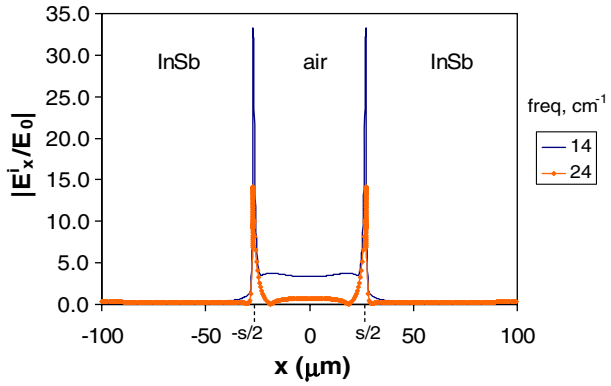

FIG. 3 (color online). Electric field enhancement, $|\frac{E_x^i}{E_0}|$, as a function of x (μm) with $d = 381$ μm, $s = 55$ μm and $h = 4$ μm, for $\lambda = 714$ and 417 μm. Note the majority of the enhancement takes place at the slot edges, i.e., around $(-s/2)$ and $(s/2)$.

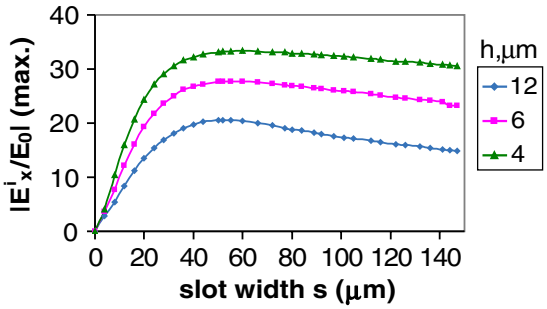

FIG. 4 (color online). Plot of maximum electric field enhancement, $|\frac{E_x^i}{E_0}|$(max.), at the incident interface and around slot edges, as a function of s (μm) with $d = 381$ μm and $\lambda = 714$ μm, for different h values ($h = 12$, 6, and 4 μm).

range. The z component is negligibly small in the entire slot region except around the edges, which confirms the approximate TEM mode in the slot region. The enhancement mechanism cannot be attributed to a surface plasmon mode since the plasmon matching condition [6] is not appropriate for permittivities with substantial imaginary parts and for structures with small thickness ($h \ll \lambda$).

Figure 4 shows the plot of maximum electric field enhancement, $|\frac{E_x^i}{E_0}|$(max.), at the incident interface and slot edges, as a function of slot width s (μm), for different h values (μm) and a constant periodicity, d (at 14 cm^{-1}). It is clear that the enhancement has a maximum around the ratio s:d equal to 1:7 and does not change significantly with further increase of slot width.

In summary, modeling a subwavelength array of slots in InSb films yielded strong electric field edge effects in propagation of THz radiation through the periodic structure. A reasonable level of transmission (0.15 for $h =$ 12 μm) was obtained, with no anomalies as a function of frequency. Such strongly enhanced local electromagnetic fields near slot edges can potentially be used for the development of novel biophotonic sensors with the radiation to biomaterial coupling enhancement factors on the order of 1000, leading to a substantial increase in detection sensitivity. Another possible application is monitoring changes of dielectric properties of biomaterials [29,30] in biophysical processes, for example, denaturation of DNA.

This work was funded by a grant from the W. M. Keck foundation. Student support from the NSF CBET Grant No. 0403963 is also acknowledged.

*Electronic address: gb7k@virginia.edu

[1] T. Globus, D. Woolard, M. Bykhovskaia, B. Gelmont, L. Werbos, and A. Samuels, Int. J. High Speed Electronics Systems **13**, 903 (2003).
[2] T. Globus, D. Woolard, T. W. Crowe, T. Khromova, B. Gelmont, and J. Hesler, J. Phys. D **39**, 3405 (2006).
[3] A. Bykhovski, T. Globus, T. Khromova, B. Gelmont, and D. Woolard, Proc. SPIE-Int. Soc. Opt. Eng. **6212**, 62 120H (2006).
[4] M. E. McDonald, A. Alexanian, R. A. York, Z. Popovic, and E. N. Grossman, IEEE Trans. Microwave Theory Tech. **48**, 712 (2000).
[5] *Electromagnetic Theory of Gratings*, edited by R. Petit (Springer-Verlag, Berlin, Heidelberg, 1980).
[6] P. Sheng, R. S. Stepleman, and P. N. Sanda, Phys. Rev. B **26**, 2907 (1982).
[7] H. E. Went, A. P. Hibbins, J. R. Sambles, C. R. Lawrence, and A. P. Crick, Appl. Phys. Lett. **77**, 2789 (2000).
[8] Q. Cao and P. Lalanne, Phys. Rev. Lett. **88**, 057403 (2002).
[9] T. W. Ebbesen, H. J. Lezec, H. F. Ghaemi, T. Thio, and P. A. Wolff, Nature (London) **391**, 667 (1998).
[10] H. F. Ghaemi, T. Thio, D. E. Grupp, T. W. Ebbesen, and H. J. Lezec, Phys. Rev. B **58**, 6779 (1998).
[11] T. Thio, H. F. Ghaemi, H. J. Lezec, P. A. Wolff, and T. W. Ebbesen, J. Opt. Soc. Am. B **16**, 1743 (1999).
[12] E. Popov, M. Neviere, S. Enoch, and R. Reinisch, Phys. Rev. B **62**, 16 100 (2000).
[13] L. Martin-Moreno, F. J. Garcia-Vidal, H. J. Lezec, K. M. Pellerin, T. Thio, J. B. Pendry, and T. W. Ebbesen, Phys. Rev. Lett. **86**, 1114 (2001).
[14] S. A. Darmanyan and A. V. Zayats, Phys. Rev. B **67**, 035424 (2003).
[15] S. H. Chang and S. K. Gray, Opt. Express **13**, 3150 (2005).
[16] H. Cao and A. Nahata, Opt. Express **12**, 1004 (2004).
[17] D. Qu, D. Grischkowsky, and W. Zhang, Opt. Lett. **29**, 896 (2004).
[18] J. Gomez Rivas, C. Schotsch, P. Haring Bolivar, and H. Kurz, Phys. Rev. B **68**, 201306(R) (2003).
[19] J. Gomez Rivas, C. Janke, P. Haring Bolivar, and H. Kurz, Opt. Express **13**, 847 (2005).
[20] H. Raether, *Surface Plasmons on Smooth and Rough Surfaces and on Gratings*, Springer Tracts in Modern Physics Vol. 111 (Springer-Verlag, Berlin, 1988), Chap. 2, p. 4.
[21] J. A. Porto, F. J. Garcia-Vidal, and J. B. Pendry, Phys. Rev. Lett. **83**, 2845 (1999).
[22] F. J. Garcia-Vidal and L. Martin-Moreno, Phys. Rev. B **66**, 155412 (2002).
[23] G. B. Arfken and H. J. Weber, *Mathematical Methods for Physicists* (Academic, San Diego, CA, 1995), 4th ed., Chap. 14, p. 836.
[24] E. Popov, S. Enoch, G. Tayeb, M. Neviere, B. Gralak, and N. Bonod, Appl. Opt. **43**, 999 (2004).
[25] D. G. Esaev, M. B. M. Rinzan, S. G. Matzik, and A. G. U. Perera, J. Appl. Phys. **96**, 4588 (2004).
[26] J. S. Blakemore, J. Appl. Phys. **53**, R123 (1982).
[27] E. Litwin-Staszewska, W. Szymanska, and P. Piotrzkowski, Phys. Status Solidi B **106**, 551 (1981).
[28] J. D. Jackson, *Classical Electrodynamics* (John Wiley & Sons, New York, 1975), 2nd ed., Chap. 2, p. 77.
[29] R. Parthasarathy, T. Globus, T. Khromova, N. Swami, and D. Woolard, Appl. Phys. Lett. **87**, 113901 (2005).
[30] N. S. Swami, C. F. Chou, and R. Terberueggen, Langmuir **21**, 1937 (2005).